Composition dependent magnetic properties of iron oxide-polyaniline nanoclusters

著者	SHARMA PARMANAND
journal or publication title	Journal of Applied Physics
volume	97
number	1
page range	014311-1-014311-6
year	2005
URL	http://hdl.handle.net/10097/47375

doi: 10.1063/1.1829788

Composition dependent magnetic properties of iron oxide-polyaniline nanoclusters

Raksha Sharma, Subhalakshmi Lamba, and S. Annapoorni[a)]
Department of Physics and Astrophysics, Delhi University, Delhi 110007, India

Parmanand Sharma
Japan Science and Technology Agency, Sendai 980-8577, Japan

Akihisa Inoue
Institute for Materials Research, Tohoku University, Sendai 980-8577, Japan

(Received 22 July 2004; accepted 13 October 2004; published online 14 December 2004)

γ-Fe_2O_3 prepared by sol gel process was used to produce nanocomposites with polyaniline of varying aniline concentrations. Transmission electron microscopy (TEM) shows the presence of chain like structure for lower polyaniline concentration. The room temperature hysteresis curves show finite coercivity of ~160 Oe for all the composites, while the saturation magnetization was found to decrease with increasing polymer content. Zero field cooled-field cooled magnetization measurements indicate high blocking temperatures. It is believed that this indicates a strongly interacting system, which is also shown by our TEM results. Monte Carlo simulations performed on a random anisotropy model with dipolar and exchange interactions match well with experimental results. © *2005 American Institute of Physics*. [DOI: 10.1063/1.1829788]

I. INTRODUCTION

Nanostructured materials have attracted a lot of attention due to their commercial exploitation as sensors, batteries, toners in photocopying, quantum electronic devices, smart windows, and memory applications. Nanostructured magnetic materials are now being extensively studied for high capacity magnetic storage media, integrated circuits, color imaging, magnetic refrigeration, biomedical application and spintronics.[1–5] The agglomeration in these magnetic nanoparticles due to Vander Waal's and magnetostatic interparticle interaction hampers their use for technological applications. Several methods have been employed to reduce this problem of agglomeration, namely, blending colloidal nanomagnetic particles with polymers, coating of oxide particles with polymers like polyvinyl alchohol, polyvinylpyrrolidone, polymethylmethacrylate, etc., forming a core shell structure or embedding the particles in a polymer matrix.[6–9] These so called nanocomposites are also used in blend with conducting polymers like polypyrrole (PPy), polyaniline (PANI), etc.

Iron oxide-conducting polymer core shell nanocomposites which exhibit the properties of both constituents, i.e., magnetic as well as conducting, have proved to be a useful material for many applications like electromagnetic shielding, gas and humidity sensors, etc.[10] Magnetic investigations on γ-Fe_2O_3–PPy nanocomposites[11] reveal that the size and, hence, the magnetic properties can be controlled by varying the PPy content in the nanocomposite.

The properties of fine particle magnetic systems are known to be strongly dependent on the size, anisotropy, and interactions like the exchange and dipolar.[12,13] The effect of interparticle interactions in magnetic nanoparticle systems has been investigated by different authors.[14,15] In magnetic nanocomposites these factors are easily controlled by varying the composition of the polymer. Hence, it is seen that all the magnetic properties of these systems are sensitive to polymer concentration. Our earlier investigations on the γ-Fe_2O_3 polypyrrole nanocomposites reveal that superparamagnetic thresholds as evidenced by the presence of blocking are very high even for fairly small particles. Our numerical simulations based on the random anisotropy, interacting model for single domain magnetic particle arrays also show that for a system with exchange interactions, as possible in a nanocomposite, has fairly high blocking even for particles sizes ~10–15 nm.[16]

In this article we report the preparation of magnetic nanocomposites of polyaniline and iron oxide. In order to determine the size, composition, structural, and magnetic properties of the nanocomposite several investigations viz. transmission electron microscopy (TEM) Fourier-transform infrared spectroscopy (FTIR), x-ray diffraction (XRD), hysteresis measurements and the low field (applied field of 25 and 100 Oe) zero field cooled-field cooled (ZFC–FC) magnetization measurements have been carried out. We also perform Monte Carlo simulations on the interacting random anisotropy model using certain parameters derived from our experimental results, like the particle size and interparticle separation. The purpose of the simulation is to estimate the strength of typical exchange and anisotropy energies in this system.

In Sec. II we describe the method of preparation, in Sec. III we present the characterization results. In Sec. IV we present the magnetization studies, in Sec. V we describe the method and results of our simulation studies, and in Sec. VI we present our conclusions.

[a)]Electronic mail: annapoorni@physics.du.ac.in

II. EXPERIMENTAL SYNTHESIS

The γ-Fe_2O_3 nanoparticles were synthesized by sol gel process using ferric nitrate $[Fe(NO_3)_3 \cdot 9H_2O]$ as precursor and 2-methoxy ethanol as solvent.[11] These particles were further dispersed in a mixture of 10 cm^3 de-ionized water, 50 cm^3 of 1 M HCl and 0.4 cm^3 (0.39 gm) of aniline monomer. The earlier solution was continuously stirred for 1 h at ice temperature before adding the oxidant. Agitation due to stirring reduces the agglomeration by breaking the big clusters into smaller ones. On addition of oxidant prepared by dissolving ammonium persulphate (1 gm) in 20 ml distilled water at a rate of 0.08 ml/min, simultaneous polymerization and stirring leads to coating of PANI chains on these smaller γ-Fe_2O_3 particles. The reaction was continued for 4 h with the solution placed in an ice water bath, after which it was filtered and washed repeatedly with 1 M HCl until the disappearance of the color of the filtrate. Subsequently it was washed with methanol and diethyl ether. The powder was allowed to dry at room temperature for 48 h. It was observed that the color of the powder thus obtained for different concentrations of γ-Fe_2O_3: aniline monomer (like 1:0, 1:0.05, 1:0.1, 1:0.2, and 1:0.4) changed from brown to dark green as the concentration of aniline monomer was increased. This shows the presence of a higher concentration of the polymer in the composite since pure PANI in its doped form is dark green in color.

The crystal structure of the powder was examined by a Rigaku Rotaflex diffractometer using a Cu $K\alpha$ ($\lambda = 1.5918$ Å) at 40 keV. The size and shape of the particles were analyzed by a JEOL JEM 2000 EX TEM. The presence of the polymer was confirmed using a Nicolet 510 P FTIR spectrometer. A Quantum Design MPMS-5S Quantum Design superconducting quantum information device magnetometer was used for magnetic characterization in the temperature range of 5–310 K. For the ZFC measurements the sample was cooled down to 5 K in the absence of an external magnetic field followed by measurements in a constant magnetic field during the warming run of the experiments. In the FC measurements, the sample was cooled from 310 down to 5 K in the presence of the same constant magnetic field which was also used in the subsequent warm up scan. The room temperature (~300 K) hysteresis loop $M(H)$ was measured using a vibrating sample magnetometer (VSM-5, TOEI Industry Co. Ltd., Tokyo, Japan), and the samples were subjected to a magnetic field cycling between +1.5 and −1.5 T.

III. RESULTS AND DISCUSSION

A. X-ray diffraction

Figures 1(a)–1(d) show the XRD pattern of different compositions of the γ-Fe_2O_3:PANI composite, unannealed, in varying ratios viz. 1:0, 1:0.1, 1:0.4 and 0:1 (pure PANI). Peaks were observed at $2\theta = 30.360$, 33.982, 35.691, and 57.400, with *hkl* values (206), (109), (119), and $(11\bar{1}5)$ which corresponds to the γ-Fe_2O_3 phase. The lattice constant was calculated to be $a = 8.3452 \pm 0.0001$ Å, which compares well with the literature value of 8.34 Å.[17] It was observed that with increase in concentration of PANI the intensity of peaks decreases and also some low intensity peaks are suppressed. This can be explained by the thicker coating of PANI on iron oxide which suppresses the peaks at higher concentrations. But it can be seen that the same phase of iron oxide is retained in all the concentrations. For pure PANI an amorphous nature is observed.

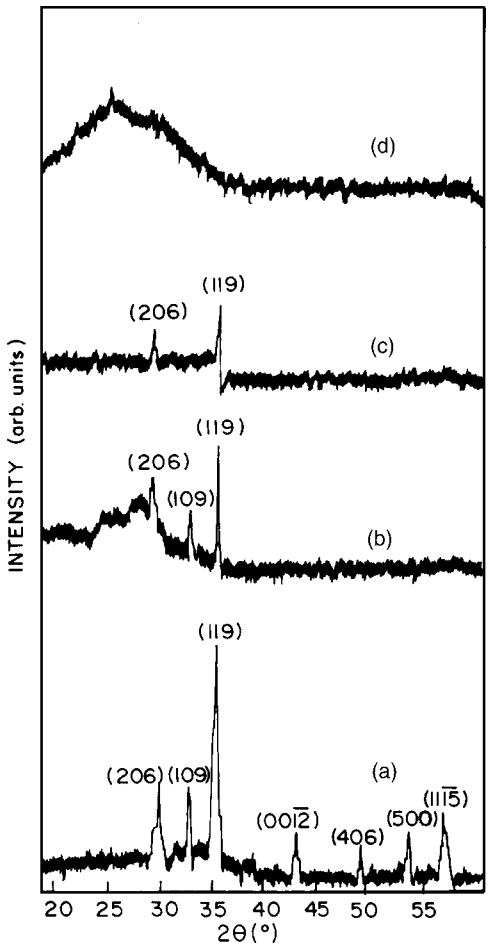

FIG. 1. X-ray diffraction for (a) pure unannealed γ-Fe_2O_3 and two different compositions of γ-Fe_2O_3–PANI nanocomposites which are (b) 1:0.1, (c) 1:0.4, and (d) pure PANI.

B. Transmission electron microscopy

The TEM in Fig. 2(a) of unannealed iron oxide shows agglomerated clusters of iron oxide. In the presence of polymer the particle size reduces drastically as can be seen from Fig. 2(b) which is a composite in the ratio 1:0.1, i.e., a low concentration of polymer. The presence of polymer prevents agglomeration of the iron oxide and hence smaller clusters are observed for composites. There is still some agglomeration present due to the partial coating of the polymer. As the polymer concentration is doubled (1:0.2) the γ-Fe_2O_3 particles were found to align in a chain as seen in Fig. 2(c). On further increasing polymer concentration intrachain structure starts building up, which is seen in Fig. 2(d) which has a composition of 1:0.4. However, the size of the particle is found to reduce further.

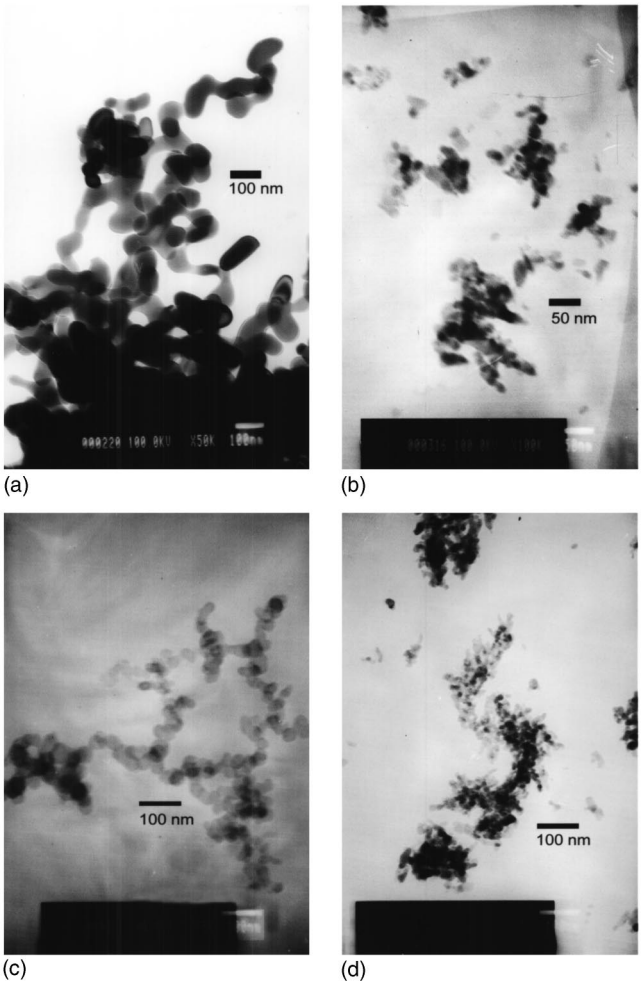

FIG. 2. TEM for (a) pure unannealed γ-Fe_2O_3 and three different compositions of γ-Fe_2O_3–PANI nanocomposites which are (b) 1:0.1, (c) 1:0.2, and (d) 1:0.4.

IV. MAGNETIZATION MEASUREMENTS

In Fig. 3 we present the hysteresis measurements performed at room temperature for three different compositions. It is seen that the magnetic nanocomposites show a finite coercivity at room temperature for all the concentrations. This indicates that the system is still in the ferromagnetic regime, in spite of the small particle sizes. All the three systems show a tendency to saturate at 15 kOe and the coercivities are in the range of 160 Oe. The saturation magnetization M_S are found to be 53.37, 44.29, and 35.31 emu/gm for concentrations of 1:0.1, 1:0.2, and 1:0.4, respectively, while the corresponding retentivities are ~8.5, 7, and 5.9 emu/gm. The reduced value of the saturation magnetization for increasing polymer concentration is expected, due the presence of smaller quantities of γ-Fe_2O_3 in the sample. In the inset we have plotted the same data in the field range of −2 to 2 kOe. The value of the coercivity is almost the same for all the concentrations indicating that the anisotropy energy of the magnetic particles is not much affected by the presence of polymer. The low value of the coercivity indicates that the system is close to superparamagnetic behavior.

In order to confirm the onset of the superparamagnetic phase, ZFC–FC magnetization measurements were performed for one of the above samples viz. 1:0.4 for which the particle sizes seem to be very small [Fig. 2(d)] and the results are shown in Fig. 4. The measurements are performed at two different field strengths of 25 [curve (a)] and 100 Oe [curve (b)]. At 100 Oe the system seems to be closer to blocking at 300 K than at 25 Oe. From our TEM (Fig. 2) it is clear that the particle sizes decrease with increasing proportion of PANI in the composite. Hence, it is expected that for the lower concentration sample the blocking temperature would be even higher than room temperature.

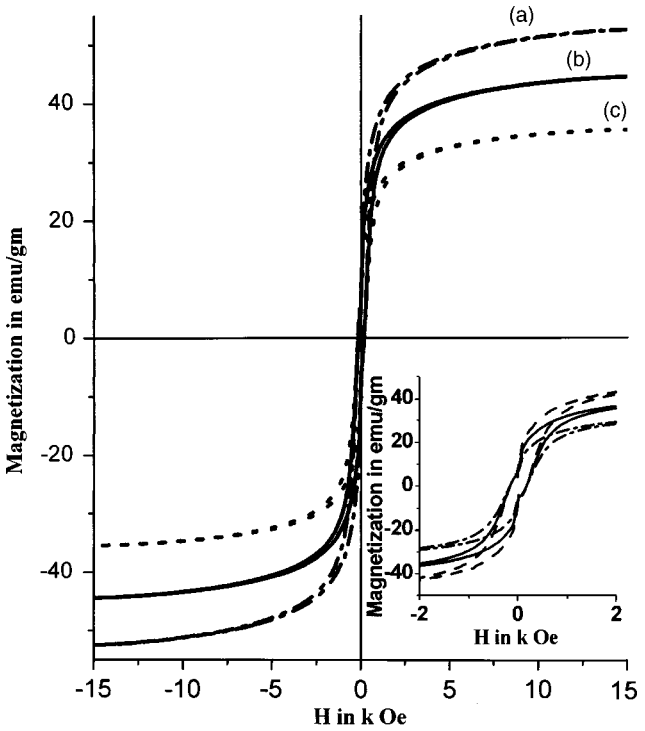

FIG. 3. Experimental hysteresis at 300 K for three different compositions of γ-Fe_2O_3–PANI nanocomposites which are (a) 1:0.1, (b) 1:0.2, and (c) 1: 0.4. Inset shows the data plotted over the low field range.

It is our belief that for systems of magnetic oxide nanoparticles which have a tendency to cluster, the blocking temperatures is not only decided by the particle size and anisotropy constant but also the exchange and dipolar interactions. Large exchange interactions have a tendency to increase the blocking temperature, which we feel may be the case in these systems. A better understanding of these clusters can be obtained by studying the dilute magnetic nanocomposites.

V. SIMULATION AND RESULTS

The simulation is performed with an array of N single domain magnetic particles positioned randomly in a cube of side L. Each particle has a magnetic moment vector $\boldsymbol{\mu}_i$ and the direction of the easy axis of magnetization of the particle is represented by the unit vector $\mathbf{n}_i$. The magnetic moment vector for a single particle has a temperature independent value $\boldsymbol{\mu}_i = V_i M_S \boldsymbol{\sigma}_i$ where M_S is the saturation magnetization and $\boldsymbol{\sigma}_i$ is the unit vector along the direction of magnetization. The volume of the particle V_i is picked from a normal distribution $P(V)dV = [1/(2\pi t^2)^{1/2}]\exp[-(V-V_0)^2/2t^2]$ where V_0 represents the mean volume of the particle and t is the

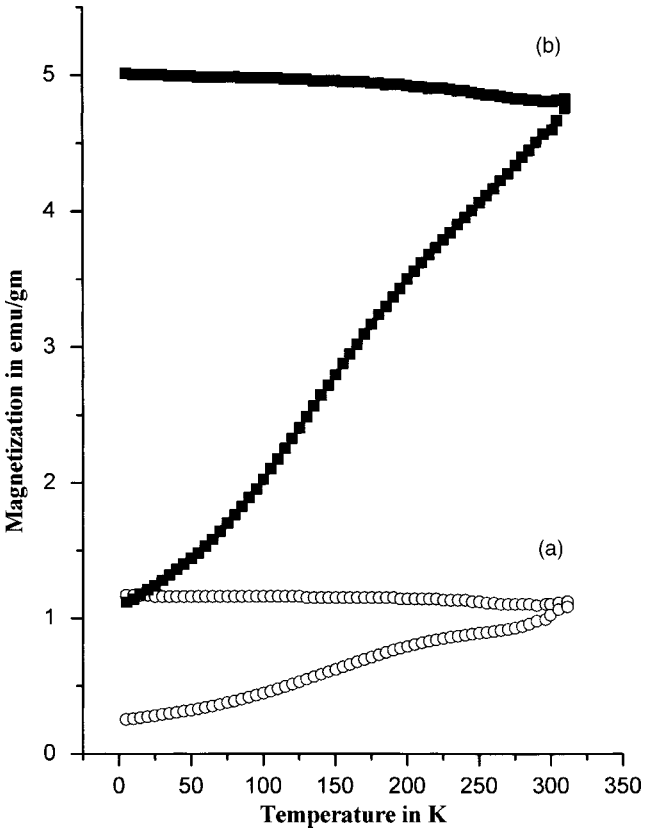

FIG. 4. Experimental ZFC–FC magnetization results for 1:0.4 composition of γ-Fe_2O_3–PANI nanocomposite at (a) 25 and (b) 100 Oe.

width of the distribution which is taken to be 0.1. This is to account for the experimental results which show that the magnetic nanoparticles in the sample are (i) not all of the same shape and size and (ii) positioned randomly in the sample. The directions of the easy axis of magnetization of each particle is picked randomly, keeping in mind that the particles could have different shapes. Such an array of interacting single domain magnetic nanoparticles can be described using the following Hamiltonian[18]

$$H = -K\sum_i V_i \frac{(\boldsymbol{\mu}_i \cdot \mathbf{n}_i)^2}{|\boldsymbol{\mu}_i|^2} - \sum_{\langle i \neq j \rangle} J_{ij} \boldsymbol{\mu}_i \cdot \boldsymbol{\mu}_j - \mu_0 \sum_{\langle i \neq j \rangle} \frac{3(\boldsymbol{\mu}_i \cdot \mathbf{e}_{ij})(\boldsymbol{\mu}_j \cdot \mathbf{e}_{ij}) - \boldsymbol{\mu}_i \cdot \boldsymbol{\mu}_j}{r_{ij}^3} - \mu_0 \sum_j \mathbf{H} \cdot \boldsymbol{\mu}_j. \tag{1}$$

The first term in Eq. (1) represents the anisotropy energy of the *i*th magnetic particle which has an anisotropy constant *K*. The second term is the exchange interaction energy between the different particles in the array and J_{ij} is the strength of the ferromagnetic exchange interaction between two particles with localized magnetic moment vectors $\boldsymbol{\mu}_i$ and $\boldsymbol{\mu}_j$, respectively. The third term is the dipolar interaction between these particles, with r_{ij} as the distance between the *i*th and *j*th particles and $\mathbf{e}_{ij}$ the unit vector pointing along $\mathbf{r}_{ij}$. The last term is the energy of the particles due to an externally applied magnetic field *H*. For the purpose of simulation we assume that the exchange interaction has a site independent constant value $J_{\text{eff}}=J$.

Magnetization studies (FC–ZFC) show that the blocking temperatures are very high, which is evident even in the hysteresis measurements. Our earlier simulations[16] suggest that the shape of the hysteresis curve (Fig. 3) is typical of a system in which both exchange and dipolar interactions play a role. It is not possible to derive the value of either *K* or *J* from any of our experimental results. So for our simulation we use as an input the particle size and the typical interparticle distance, and try to obtain the experimentally observed coercivity and retentivity by varying the value of *K* and *J*. We work with a system of $N=64$ particles. The mean volume V_0 is taken to be equivalent to that of a sphere of radius $r_i = 7.5$ nm. The dipolar interaction energy is calculated by summing over periodic repeats of the basic simulation cell by the method of Lekner summation.[19] The simulation of the hysteresis is performed at a temperature of 300 K by the Monte Carlo method using the standard Metropolis algorithm.[16,20,21] The simulation is started at a very low field along the *z* axis of the simulation cube, using an ensemble of magnetization vectors for the array, which gives a net magnetization of zero along the *z* direction. The system is saturated by gradually increasing the magnetic field up to a very high field which is sufficiently higher than its anisotropy field (in this case 1.5 T). Then the magnetic hysteresis loop is simulated. For each value of the magnetic field 10 000 Monte Carlo steps are used for the thermalization of the system and the calculation of the net magnetization along the field direction is made over the next 5000 Monte Carlo steps. The results are averaged over five initial configurations of the magnetic particles (position, magnetization and easy axes directions). The values of $M_S = 4\times10^5$ A/m for γ-Fe_2O_3 is taken from literature. To fit to the experimentally observed values of the coercivity and retentivity in these systems, we find that the anisotropy constant should be higher than for the pure γ-Fe_2O_3 system which is $\sim 0.045\times10^5$ J/m^3. A good fit to the experimental results are obtained for a much higher value of the anisotropy constant which is $K=0.75\times10^5$ J/m^3 and a value of $J=0.02E_A$, where the mean anisotropy energy $E_A=KV_0$. The values of the anisotropy constant calculated from ac susceptibility measurements performed on coated superparamagnetic iron oxide nanoparticles shows that the values of *K* are sensitive to the coating material, and for small particles of γ-Fe_2O_3 and Fe_3O_4 can be an order of magnitude larger than the values for bulk, in fact high as $2-4\times10^5$ J/m^3.[22,23] So the value of *K* estimated from the simulation is well within the experimentally reported limits for coated experimental oxides. In Fig. 5 we show the results of the hysteresis simulations, by plotting the scaled magnetization M/M_S with the applied field, for three different values of the anisotropy constant keeping V_0, the interparticle distance and the exchange interaction same for all three curves. Curve (a) is the experimental plot at 300 K for the γ-Fe_2O_3–PANI concentration of 1:0.4. It is seen that the closest fit to the experimental curve is for a value of $K=0.75\times10^5$ J/m^3 which is curve (c). For $K=1.25\times10^5$ J/m^3 which is curve (d), the coercivity is much larger than that observed experimentally and for $K=0.25\times10^5$ J/m^3 [curve (d)] the coercivity is 0 indicating the system is already superparamagnetic at 300 K.

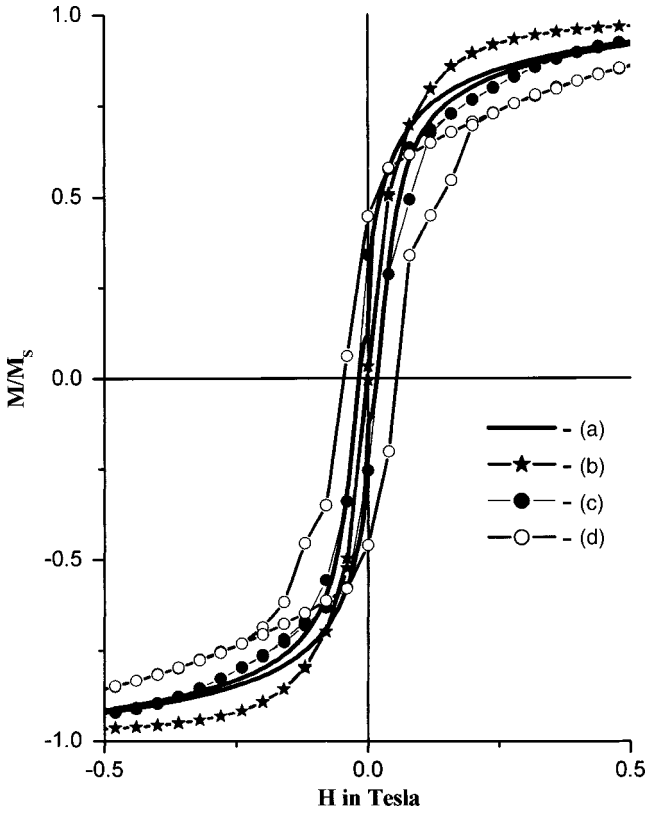

FIG. 5. (a) Experimental hysteresis at 300 K for 1:0.4 composition of γ-Fe_2O_3–PANI composition and simulated hysteresis curves at 300 K for $J=0.02E_A$ and (b) $K=0.25\times10^5$ J/m^3, (c) $K=0.75\times10^5$ J/m^3, and (d) $K=1.25\times10^5$ J/m^3.

Using the same parameters and the value of $K=0.75\times10^5$ J/m^3 which is closest to the experimental curve, we simulate the FC–ZFC magnetization curves which are shown in Fig. 6. The effect of a large K is that the blocking temperature $\sim$325 K for $H=100$ Oe, which again is in good agreement with the experimental result (Fig. 4), indicating that the values of K and J estimated from the hysteresis simulation are appropriate for the system being studied. The inset shows the variation of the blocking temperature with increasing applied field. As the field is changed from 0.0025 to 0.01 T, T_B changes from 360 to 325 K. This is in keeping with the experimental trend (Fig. 4). The reasons for the high blocking temperatures even for such small particles are the presence of interactions. The broadness of the ZFC peak is indicative of the size distribution in the sample.

It is seen that the magnetization in the low temperature range in Fig. 6 is less than that seen experimentally. This is because of the high value of the anisotropy constant and the exchange parameter ($J=0.02E_A$) which is chosen in keeping with the room temperature coercivity observed experimentally. If the exchange parameter is increased for the simulation, the low temperature magnetization value is found to increase. It is known that the low temperature behavior of magnetic fine particles is very sensitive to competing effects like the anisotropy, and interactions like the dipolar and exchange, which we are in the process of examining by studying dilute magnetic systems.

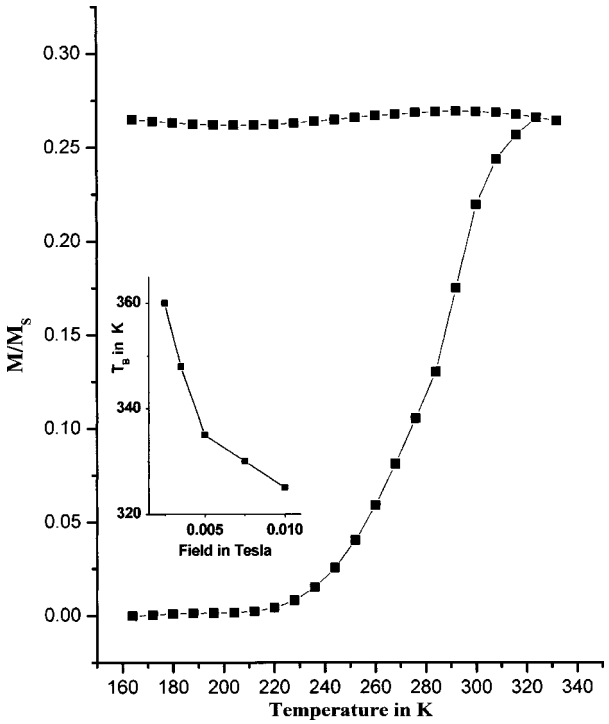

FIG. 6. (a) Simulated ZFC–FC magnetization curves for $J=0.02E_A$, $K=0.75\times10^5$ J/m^3, and $H=0.01$ T. Inset shows the variation of the blocking temperature T_B with the magnetic field in Tesla.

VI. CONCLUSIONS

Our experiments indicate that for fairly low concentrations of polyaniline in the nanocomposite, we are able to obtain large variation in the particle size and magnetic properties. The particle sizes are small and even at such low concentrations of polyaniline there is less agglomeration. High blocking temperatures as confirmed by hysteresis and ZFC–FC magnetization measurements indicates that the system is in the ferromagnetic phase at room temperature. However, the low value of coercivity suggests that the system is close to superparamagnetic behavior. We are further investigating the electrical properties, like the conductivity and the dielectric behavior of these nanocomposites to understand the contribution of the polymer in the system.

ACKNOWLEDGMENTS

One of the authors (R.S.) wishes to acknowledge Council of Scientific and Industrial Research (CSIR), India for financial support. The authors wish to acknowledge the Department of Science and Technology (DST), India for their financial assistance through their project (SR/S5/NM-52/2002) from their Nanoscience and Technology Initiative programme. They also acknowledge the help extended by Dr. N. C. Mehra and Dr. S. K. Shukla at the University Science and Instrumentation Centre, University of Delhi.

[1]F. J. Himpsel, J. Phys.: Condens. Matter **11**, 9483 (1999).
[2]P. Moriarty, Rep. Prog. Phys. **64**, 297 (2001).
[3]N. M. White and J. D. Turner, Meas. Sci. Technol. **8**, 1 (1997).
[4]D. A. Thompson and J. S. Best, IBM J. Res. Dev. **44**, 311 (2000).
[5]P. Sharma, A. Gupta, K. V. Rao, F. J. Owens, R. Ahuja, J. M. O. Guillen, B. Johansson, and G. A. Gehring, Nat. Mater. **2**, 673 (2003).
[6]L. Chen, W.-J. Yang, and C.-Z. Yang, J. Mater. Sci. **32**, 3571 (1997).

[7]D. K. Lee, Y. S. Kang, C. S. Lee, and P. Stroeve, J. Phys. Chem. B **106**, 7267 (2002).
[8]S. Maeda and S. P. Armes, J. Mater. Chem. **4**, 935 (1994).
[9]C. L. Huang and E. Matijevic, J. Mater. Res. **10**, 1327 (1995).
[10]K. Suri, S. Annapoorni, A. K. Sarkar, and R. P. Tandon, Sens. Actuators B **81**, 277 (2002).
[11]K. Suri, S. Annapoorni, R. P. Tandon, and N. C. Mehra, Synth. Met. **126**, 137 (2002).
[12]*Magnetic Properties of Fine Particles*, edited by J. H. Dormann and D. Fiorani (North Holland, Amsterdam, 1992).
[13]D. Fiorani *et al.*, J. Magn. Magn. Mater. **196–197**, 143 (1999).
[14]C. Papusoi, Jr., J. Magn. Magn. Mater. **195**, 708 (1999).
[15]D. Hinzke and U. Nowak, Phys. Rev. B **61**, 6734 (2000).
[16]S. Lamba and S. Annapoorni, Eur. Phys. J. B **39**, 19 (2004).
[17]International Centre for Diffraction Data (1979), Inorganic Vol. PDIS-20iRB, Publ. JCPDS.
[18]J. J. Weis, J. Phys.: Condens. Matter **15**, S1471 (2003).
[19]J. Lekner, J. Phys. A **176**, 485 (1991).
[20]L. Wang, J. Ding, H. Z. Kong, Y. Li, and Y. P. Feng, Phys. Rev. B **64**, 214410 (2001).
[21]K. Binder, H. Rauch, and V. Wildpaner, J. Phys. Chem. Solids **31**, 391 (1970).
[22]S. Morup and H. Topsoe, Appl. Phys. **11**, 63 (1976).
[23]B. J. Jonsson, T. Turkki, V. Strom, M. S. El-Shall, and K. V. Rao, J. Appl. Phys. **79**, 5063 (1996).